

Published in final edited form as:

*Am J Physiol Cell Physiol*. 2003 May ; 284(5): C1114–C1122. doi:10.1152/ajpcell.00400.2002.

## **$HCO_3^-$ -dependent soluble adenylyl cyclase activates cystic fibrosis transmembrane conductance regulator in corneal endothelium**

Xing Cai Sun<sup>1</sup>, Chang-Bin Zhai<sup>1</sup>, Miao Cui<sup>1</sup>, Yanqiu Chen<sup>2</sup>, Lonny R. Levin<sup>2</sup>, Jochen Buck<sup>2</sup>, and Joseph A. Bonanno<sup>1</sup>

<sup>1</sup>School of Optometry, Indiana University, Bloomington, Indiana 47405

<sup>2</sup>Department of Pharmacology, Weill Medical College of Cornell University, New York, New York 10021

### **Abstract**

$HCO_3^-$ -dependent soluble adenylyl cyclase activates cystic fibrosis transmembrane conductance regulator in corneal endothelium. *Am J Physiol Cell Physiol* 284: C1114–C1122, 2003. First published January 8, 2003; 10.1152/ajpcell.00400.2002.— cAMP-dependent activation of the cystic fibrosis transmembrane conductance regulator (CFTR) regulates fluid transport in many tissues. Secretion by the corneal endothelium is stimulated by cAMP and dependent on  $HCO_3^-$ . We asked whether  $HCO_3^-$  can secondarily increase CFTR permeability in bovine corneal endothelial cells (BCEC) by activating soluble adenylyl cyclase (sAC). Immunofluorescence suggests that sAC is distributed throughout the cytoplasm.  $HCO_3^-$  (40 mM) increased cAMP concentration 42% in the presence of 50  $\mu$ M rolipram (a phosphodiesterase 4 inhibitor), and a standard  $HCO_3^-$  Ringer solution (28.5 mM) increased apical  $Cl^-$  permeability by 78% relative to  $HCO_3^-$ -free solution. The  $HCO_3^-$ -dependent increase in  $Cl^-$  permeability was reduced 60% by 20 mM  $NaHSO_3$  (a weak agonist of sAC).  $NaHSO_3$  alone increased apical  $Cl^-$  permeability by only 13%. The  $HCO_3^-$ -dependent increase in  $Cl^-$  permeability was reduced 57% in the presence of 50  $\mu$ M Rp-adenosine 3',5'-cyclic monophosphorothioate, and 86% by 50  $\mu$ M 5-nitro-2-(3-phenylpropyl-amino)benzoic acid but unaffected by 200  $\mu$ M apical  $H_2DIDS$ . CFTR phosphorylation was increased 23, 150, and 32% by 20 mM  $HSO_3^-$ , 28.5 mM  $HCO_3^-$ , and 28.5 mM  $HCO_3^-$  + 20 mM  $HSO_3^-$ , respectively. Activation of apical  $Cl^-$  permeability by 5  $\mu$ M genistein was increased synergistically by  $HCO_3^-$  over that due to genistein and  $HCO_3^-$  alone. We conclude that  $HCO_3^-$ -stimulated sAC is a form of autocrine signaling that contributes to baseline cAMP production, thereby affecting baseline CFTR activity in BCEC. This form of autocrine signaling may be important in tissues that express sAC and exhibit robust  $HCO_3^-$  influx (e.g., ocular ciliary epithelium, choroid plexus, and airway epithelium).

## Keywords

chloride transport; cAMP; CFTR phosphorylation

THE CORNEAL ENDOTHELIUM MAINTAINS the hydration and optical transparency of the cornea by continuously secreting fluid in opposition to a leak driven by tissue swelling pressure generated by stromal glycosaminoglycans. Endothelial fluid secretion is dependent on the presence of  $HCO_3^-$  (15, 18, 34) and  $Cl^-$  (34, 47) and is slowed in the presence of carbonic anhydrase inhibitors (18, 19, 27). Tracer flux studies have shown that net basal to apical  $HCO_3^-$  (19, 21, 45) and  $Cl^-$  (21) transport can contribute to the small ( $-0.5$  mV) apical-side negative transepithelial potential; however, the relative contribution of each anion is unclear.

$HCO_3^-$  and  $Cl^-$  are taken up by corneal endothelial cells via basolateral  $Na^+-2HCO_3^-$  (NBC1; Refs. 24, 43) and  $Na^+-K^+-2Cl^-$  (NKCC1; Refs. 13, 23) cotransporters, respectively. Both intracellular  $Cl^-$  concentration ( $[Cl^-]$ , 40 mM; Ref. 6) and  $[HCO_3^-]$  (20 mM; Ref. 5) are above electrochemical equilibrium, indicating the potential for apical anion efflux through conductive channels. Recently, we determined (42) that the cystic fibrosis transmembrane conductance regulator (CFTR) is present on the apical membrane of corneal endothelial cells. Activation of CFTR by forskolin (42) or adenosine (3, 49) significantly increases apical  $Cl^-$  and  $HCO_3^-$  permeability. Similarly, increasing endothelial cAMP by application of adenosine, forskolin, or phosphodiesterase (PDE) inhibitors stimulates fluid secretion (16, 33, 35, 46). The stimulation of fluid transport by the PDE4 inhibitor rolipram (46) suggests that there is a significant basal level of adenylyl cyclase (AC) activity that is contributing to baseline fluid secretion.

One possible source of basal AC activity is the  $HCO_3^-$ -activated AC that is present in the particulate fraction of several ocular tissues including the corneal endothelium (28). This type of AC, called soluble AC (sAC), has recently been cloned and characterized (10, 12).  $HCO_3^-$  is the only known physiologically relevant agonist for sAC.  $HCO_3^-$  binds directly to and activates sAC in a pH-independent manner (12). sAC is insensitive to G protein regulation and is not activated by forskolin (8, 10), indicating that it is distinct from the transmembrane adenylyl cyclases (tmACs). sAC has been extensively characterized in mammalian sperm cells (10, 12) and is expressed in kidney and choroid plexus (36). sAC is distributed throughout the cell and appears to associate with distinct microdomains (50). Thus sAC-dependent cAMP production could affect many potential targets, which may be activated by localized increases in [cAMP]. In essence, sAC-dependent cAMP production represents a form of autocrine stimulation in cells that actively take up  $HCO_3^-$  contributing to baseline activity of cAMP-dependent processes.

In this study, we show that sAC is expressed in corneal endothelium and that the presence of  $HCO_3^-$  can increase cell [cAMP]. Furthermore, we found that the increased cAMP in the presence of  $HCO_3^-$  can stimulate apical  $Cl^-$  permeability and increase phosphorylation of CFTR. These findings indicate that, in addition to being a component of net anion transport,  $HCO_3^-$  is an agonist for cAMP production that leads to increased apical anion permeability through CFTR. Given the widespread expression of sAC (36), these findings suggest that the

baseline activity of cAMP-dependent transport can be significantly influenced by the activity of  $HCO_3^-$  transport mechanisms.

## MATERIALS AND METHODS

### Cells

Primary cultures of bovine corneal endothelial cells (BCEC) obtained from fresh cow eyes and CHO cells were grown in DMEM (44 mM  $HCO_3^-$ )-10% bovine calf serum and gassed with 7%  $CO_2$  as previously described (4). Cells were subcultured and grown to confluence on 35-mm petri dishes, glass coverslips, or permeable substrates (Anodiscs, Fisher Scientific).

### sAC mRNA expression

A pair of sAC primers was constructed on the basis of the published cDNA sequence (10). The sAC sense primer was 5'-CCTGGAATAACCTGTTCAAG-3', and the sAC antisense primer was 5'-TCTGGTCCTTGAGCCACAG-3'. The expected length of PCR products for sAC was 544 bp.

Total RNA was extracted from cultured BCEC with TRIzol reagent (Invitrogen). The RNA was DNase treated with an RNase-free DNase set (Qiagen). Reverse transcription was performed with the Superscript cDNA synthesis system (Invitrogen) and oligo(dT) primers as previously described (43, 44). PCR amplifications used the High Fidelity TaKaRa Ex *Taq* PCR System kit (TaKaRa Shuzo) with denaturation at 94°C for 3 min for 1 cycle, 35 cycles of denaturation at 94°C for 30 s, annealing at 52°C for 30 s, extension at 72°C for 45 s, and a final extension for 1 cycle at 72°C for 10 min. The PCR products were loaded onto 1% agarose gels, electrophoresed, and stained with 0.5 µg/ml ethidium bromide. PCR products were purified with a 1% low-melting-point agarose gel, inserted into pCR 4-TOPO vector (Invitrogen, San Diego, CA), and sequenced as previously described (43, 44).

### Indirect immunofluorescence

Confluent cultured BCEC on coverslips were fixed and immunostained with rabbit  $\alpha$ -middle polyclonal sAC antisera (1:100 dilution; Ref. 50) and secondary antibody conjugated to Oregon green (1:500; Molecular Probes), as previously described (42, 43). Fluorescence was observed with a standard epifluorescence microscope equipped with a cooled charge-coupled device (CCD) camera. Negative controls (no primary antibody) were included in all experiments.

### Intracellular cAMP assay

Culture medium was removed from confluent BCEC and replaced with HEPES-buffered, air-equilibrated,  $HCO_3^-$ -free DMEM for 3 h at 37°C. Cells were then placed in 0, 10, or 40 mM  $HCO_3^-$ -DMEM solutions at pH 7.1 (air equilibrated), 7.3 (5%  $CO_2$ ) and 7.55 (5%  $CO_2$ ), respectively, for 30 min with or without 50 µM rolipram (a PDE4 inhibitor). Each solution also contained 0.3 mM  $\alpha,\beta$ -methyleneadenosine 5'-diphosphate (AMP-CP, an ectonucleotidase inhibitor, to reduce  $A_{2B}$  receptor stimulation and thus background [cAMP]). Parallel controls were performed in HEPES-buffered DMEM (0  $HCO_3^-$ ) at

different bath pH values. Cells were washed with PBS, lysed in 0.1 N HCl, and cleared of debris by centrifugation. [cAMP] was measured by an enzyme immunoassay kit (R&D Systems).

### CFTR phosphorylation

Confluent cultured BCEC were incubated in  $HCO_3^-$ -free DMEM with 0.3 mM AMP-CP for 3 h at 37°C, followed by a 1-h incubation in 0, 10, or 40 mM  $HCO_3^-$  containing 0.3 mM AMP-CP with 20 nM calyculin A. Cells were then lysed in chilled RIPA lysis buffer (150 mM NaCl, 1.0% NP-40, 0.5% sodium deoxycholate, 0.1% SDS, 50 mM Tris, pH 8.0, 1 mM EDTA, 0.1 mM PMSF, 10 µg/ml leupeptin, 1 µg/ml pepstatin) and cleared by centrifugation. CFTR was immunoprecipitated (MAb directed against the COOH terminus of CFTR; R&D Systems) from 1 mg of protein from each cell lysate, separated by 8% SDS-PAGE, and transferred to a polyvinylidene difluoride (PVDF) membrane (42). The membrane was probed with rabbit anti-phospho-(Ser/Thr) PKA substrate primary antibody (1:1,000; Cell Signaling Technology) and goat anti-rabbit secondary antibody coupled to horseradish peroxidase (1:5,000; Sigma). Exposed films were scanned, and the density of equal areas of the developed bands was estimated with Un-Scan-It software (Silk Scientific, Orem, UT).

### Apical $Cl^-$ permeability

Relative changes in apical  $Cl^-$  permeability were assessed with the halide-sensitive fluorescent dye 6-methoxy-*N*-ethylquinolinium iodide (MEQ). Confluent BCEC, grown on Anodiscs, were loaded with MEQ by exposure to diH-MEQ for 10 min (42). Anodiscs were placed in a double-sided microscope perfusion chamber, and apical and basolateral compartments were independently perfused at 37°C. MEQ fluorescence (excitation:  $365 \pm 10$  nm; emission: 420–450 nm) was measured as previously described (42). Anodiscs were initially perfused with a  $Cl^-$ - and  $HCO_3^-$ -free Ringer solution (in mM: 150  $Na^+$ , 4  $K^+$ , 0.6  $Mg^{2+}$ , 1.4  $Ca^{2+}$ , 148.5  $NO_3^-$ , 2  $HPO_4^{2-}$ , 10 HEPES, 2 gluconate $^-$ , and 5 glucose, pH 7.5), and the apical side was briefly pulsed with  $Cl^-$ -rich Ringer solution (equimolar replacement of 118  $NaNO_3$  with NaCl).  $HCO_3^-$ -rich,  $Cl^-$ -free Ringer solution was then introduced (prepared by equimolar substitution of 28.5  $NaNO_3$  with  $NaHCO_3$ ; gassed with 5%  $CO_2$ , pH 7.5). The apical side was then pulsed with  $Cl^-$ -rich,  $HCO_3^-$ -rich Ringer solution. Relative changes in apical  $Cl^-$  permeability between control and experimental conditions in the same cells were determined by comparing the percent change in MEQ fluorescence ( $F/F_0$ ) after addition of  $Cl^-$ , where  $F_0$  is the fluorescence in the absence of  $Cl^-$ . The maximum slope of fluorescence change was determined by calculating the first derivative with Felix software (PTI).

### Intracellular pH

Intracellular pH ( $pH_i$ ) was measured with the pH-sensitive fluorescent dye BCECF as previously described (2, 5, 43).

### Statistics

All data are expressed as means  $\pm$  SE, and Student's paired *t*-test was used for statistical analysis at  $P < 0.05$ .

## Reagents

Oligonucleotides were obtained from Invitrogen (Carlsbad, CA). MEQ, BCECF-AM, and H<sub>2</sub>DIDS were obtained from Molecular Probes (Eugene, OR). Genistein and calyculin A were obtained from LC laboratories (Woburn, MA). All other reagents were obtained from Sigma (St. Louis, MO.).

## RESULTS

PCR amplification was performed on first-strand cDNA synthesized from cultured BCEC total RNA with specific sAC primers. Figure 1A shows that RT-PCR produced a clear, specific band at the predicted size. Sequencing analysis verified the identity as sAC. Figure 1, B and C, shows indirect immunofluorescence of sAC protein in cultured BCEC, demonstrating cytoplasmic localization and suggesting numerous focal microdomains. A previous study (28) showed that BCEC cytoplasmic extracts contain HCO<sub>3</sub><sup>-</sup>-activated AC. We tested whether HCO<sub>3</sub><sup>-</sup> could increase total cellular [cAMP] in intact cells. Figure 1D shows that addition of HCO<sub>3</sub><sup>-</sup> produced a 20% increase in [cAMP] at 10 mM HCO<sub>3</sub><sup>-</sup> that was not significantly higher at 40 mM. Figure 1D also shows that inhibiting PDE4 (50 μM rolipram) allowed cAMP to accumulate to 42% over control in 40 mM HCO<sub>3</sub><sup>-</sup> ( $n = 6$ ;  $P < 0.05$ ). The effect of HCO<sub>3</sub><sup>-</sup> on [cAMP] was not simply due to the increasing pH of the HCO<sub>3</sub><sup>-</sup> solutions, because we found that increasing bath pH from 7.1 to 7.5 in the absence of HCO<sub>3</sub><sup>-</sup> produced a decrease in [cAMP] from  $20.2 \pm 1.2$  to  $14.6 \pm 1.2$  pmol/mg protein ( $n = 6$ ). Overall, these changes in [cAMP] in the intact cells are consistent with the 56% increase in cytoplasmic AC activity produced by HCO<sub>3</sub><sup>-</sup> in BCEC extracts (28).

Compared with typical tmAC agonists (e.g., forskolin or β-adrenergic agonists), the increase in total [cAMP] in response to HCO<sub>3</sub><sup>-</sup> is modest. On the other hand, adenosine (binding to A<sub>2B</sub> receptors, activating tmACs and cAMP production) can stimulate fluid secretion in corneal endothelium (33) and Calu-3 airway cells (via CFTR activation) (20) without significantly changing total cell [cAMP], indicating that localized increases in [cAMP] at the apical membrane are responsible for the stimulation. This suggests that sAC expression and the increase in total cell [cAMP] induced by HCO<sub>3</sub><sup>-</sup>, even though small, could stimulate apical CFTR in BCEC. To test this possibility, we loaded BCEC with the halide-sensitive dye MEQ and measured the rate of fluorescence change in response to apical Cl<sup>-</sup> pulses. Both apical and basolateral sides were initially perfused with Cl<sup>-</sup>- and HCO<sub>3</sub><sup>-</sup>-free solutions. Figure 2A shows that when Cl<sup>-</sup> was added to the apical side for 90 s, a small, slow decrease in MEQ fluorescence was observed. Both sides were then bathed in Cl<sup>-</sup>-free, HCO<sub>3</sub><sup>-</sup>-rich solution for at least 5 min. The addition of HCO<sub>3</sub><sup>-</sup> initially caused a sharp increase in MEQ fluorescence followed by a slow return to steady state slightly below the baseline. The sharp increase in MEQ fluorescence represents dequenching of MEQ fluorescence due to a small increase in cell volume from basolateral Na<sup>+</sup>-2HCO<sub>3</sub><sup>-</sup> uptake (38). The subsequent decrease in MEQ fluorescence is due to regulatory volume decrease (RVD) (40) along with some dye leakage. When the fluorescence signal had stabilized, Cl<sup>-</sup> was applied to the apical side in the presence of HCO<sub>3</sub><sup>-</sup>. The decrease in MEQ fluorescence was accelerated relative to the paired controls. Figure 2B summarizes the results and shows

that the apical  $\text{Cl}^-$  permeability of BCEC was significantly increased by 78% in the presence of  $\text{HCO}_3^-$ . To test the possibility that  $\text{HCO}_3^-$  could nonspecifically affect apical  $\text{Cl}^-$  permeability in cells that do not express apical cAMP-dependent  $\text{Cl}^-$  channels, the same experiments were performed with CHO cells, which do not express apical CFTR. Figure 2, C and D, shows that apical  $\text{Cl}^-$  permeability in CHO cells is not affected by the presence of  $\text{HCO}_3^-$ .

Other than CFTR, an obvious candidate for increased apical  $\text{Cl}^-$  permeability of BCEC in the presence of  $\text{HCO}_3^-$  would be an apical anion exchanger (AE). However, extensive studies have shown that AE activity is not present in cultured BCEC (2, 7, 42, 44). Consistent with the absence of AE, we found that application of the AE inhibitor  $\text{H}_2\text{DIDS}$  (200  $\mu\text{M}$ ) on the apical side had no effect on  $\text{HCO}_3^-$ -activated  $\text{Cl}^-$  permeability (data not shown). Another possibility is stimulation of a swelling-activated  $\text{Cl}^-$  channel (SACC) (38, 39); however, this is unlikely because the volume changes were small (average increased  $F/F_0 = 1.6 \pm 2\%$ ) and RVD was complete. One property of SACCs is rapid inactivation as RVD progresses (29, 30, 40). In three trials, we pulsed apical  $\text{Cl}^-$  after addition of  $\text{HCO}_3^-$  every  $\sim 7$  min for 30 min. We found that the increased  $\text{Cl}^-$  permeability was sustained while in  $\text{HCO}_3^-$  (data not shown), indicating that SACCs do not have a significant role. Finally, it is possible that the increase in  $\text{pH}_i$  (7.15 to 7.35) that accompanies exposure to  $\text{HCO}_3^-$  (5) may increase CFTR conductance independently of the effects of  $\text{HCO}_3^-$ . However, we found that increasing  $\text{pH}_i$  from 7.12 to 7.32 in the absence of  $\text{HCO}_3^-$  did not change apical  $\text{Cl}^-$  permeability (see Table 1).

To test whether the changes in apical  $\text{Cl}^-$  permeability induced by  $\text{HCO}_3^-$  could be contributed by activation of CFTR, we first examined the sensitivity to 5-nitro-2-(3-phenylpropyl-amino)benzoic acid (NPPB), which has been shown to reduce CFTR permeability in BCEC (42). Figure 2E shows that in the presence of  $\text{HCO}_3^-$  and 50  $\mu\text{M}$  NPPB, the rate of MEQ fluorescence quenching was reduced  $\sim 86\%$  relative to  $\text{HCO}_3^-$  alone. Previously, we showed (42) that in the absence of  $\text{HCO}_3^-$ , 50  $\mu\text{M}$  NPPB slowed  $\text{Cl}^-$  uptake by only 5% in nonstimulated BCEC, indicating that the inhibitory effect of NPPB in the presence of  $\text{HCO}_3^-$  was not independent of  $\text{HCO}_3^-$ . Figure 2F summarizes these results, showing that NPPB significantly reduced  $\text{HCO}_3^-$ -activated apical  $\text{Cl}^-$  permeability. The sensitivity of  $\text{HCO}_3^-$ -dependent apical  $\text{Cl}^-$  permeability to NPPB and the insensitivity to  $\text{H}_2\text{DIDS}$  are consistent with activation of CFTR.

Activation of CFTR by a  $\text{HCO}_3^-$ -dependent increase in cAMP should also result in increased CFTR phosphorylation. Figure 3A shows a representative immunoassay for phosphorylated CFTR. This blot shows that incubation in 28.5 mM  $\text{HCO}_3^-$  increased CFTR phosphorylation by a factor of 2, relative to incubation in  $\text{HCO}_3^-$ -free medium. For comparison, 10  $\mu\text{M}$  adeno-sine and 10  $\mu\text{M}$  forskolin produced 2.5- and 4.2-fold increases in CFTR phosphorylation, respectively. To demonstrate that the  $\text{HCO}_3^-$ -induced increase in CFTR phosphorylation was caused by activation of sAC, we examined the effects of  $\text{HSO}_3^-$  on CFTR phosphorylation.  $\text{HSO}_3^-$  structurally resembles  $\text{HCO}_3^-$  and is a weak agonist of sAC (12). Figure 3A shows that 20 mM  $\text{NaHSO}_3$  alone produced a 1.23-fold increase in

CFTR phosphorylation, consistent with it being a weak agonist of sAC. Moreover, the presence of 20 mM  $\text{NaHSO}_3$  together with 28.5 mM  $\text{HCO}_3^-$  reduced CFTR phosphorylation by 58% relative to  $\text{HCO}_3^-$  alone, indicating that  $\text{HSO}_3^-$  is competing with  $\text{HCO}_3^-$  for sAC. Figure 3B summarizes the effect of incubation in increasing  $[\text{HCO}_3^-]$  on CFTR phosphorylation. These results demonstrate that increasing  $[\text{HCO}_3^-]$  significantly increases CFTR phosphorylation in a simple hyperbolic fashion within the physiological range of intracellular  $[\text{HCO}_3^-]$  (10–20 mM), which is consistent with an  $\text{EC}_{50}$  of ~25 mM that was determined for sAC in cell extracts (12). Similarly, Fig. 3B also shows the effects of varying  $[\text{HCO}_3^-]$  on apical  $\text{Cl}^-$  permeability. Although the physiological change is smaller than the relative change in phosphorylation, the overall effect of increasing  $[\text{HCO}_3^-]$  is very similar.

Forskolin (10  $\mu\text{M}$ ) was previously shown to produce a four- to fivefold increase in apical  $\text{Cl}^-$  permeability in BCEC in the absence of  $\text{HCO}_3^-$  (42). Because forskolin produces maximal cAMP-dependent stimulation of CFTR, forskolin stimulation in the presence of  $\text{HCO}_3^-$  would not be expected to be greater than that in the absence of  $\text{HCO}_3^-$  if the  $\text{HCO}_3^-$ -induced increase in apical  $\text{Cl}^-$  permeability is caused by cAMP production from sAC. In paired experiments, we found that forskolin stimulation in the presence of  $\text{HCO}_3^-$  ( $4.24 \pm 0.40$  fold increase;  $n = 14$ ) was not significantly different from that in the absence of  $\text{HCO}_3^-$  ( $4.29 \pm 0.38$ -fold), consistent with  $\text{HCO}_3^-$  acting through a cAMP/PKA-dependent mechanism.

Another signature feature of CFTR is that it can also be activated by the isoflavone genistein (1, 17, 42). Previous studies showed that activation by low [genistein] (<10  $\mu\text{M}$ ) is more effective if CFTR is already phosphorylated by PKA (22). Because  $\text{HCO}_3^-$  increased the phosphorylation of CFTR, CFTR should be more sensitive to a low concentration of genistein while in  $\text{HCO}_3^-$ . To test this, we measured the increase in apical  $\text{Cl}^-$  permeability due to 5  $\mu\text{M}$  genistein in the presence and absence of  $\text{HCO}_3^-$ . In Fig. 3C, apical and basolateral sides of BCEC were initially perfused with  $\text{Cl}^-$ - and  $\text{HCO}_3^-$ -free solutions in the presence of 0.3 mM AMP-CP (to reduce background CFTR phosphorylation from endogenous adenosine stimulation). When  $\text{Cl}^-$  was added on the apical side, there was a small drop in MEQ fluorescence, which was significantly accelerated by the addition of 5  $\mu\text{M}$  genistein. After a 10-min wash with  $\text{Cl}^-$ -free and  $\text{HCO}_3^-$ -free solutions on both sides,  $\text{HCO}_3^-$  was introduced to both sides for 5 min followed by a  $\text{Cl}^-$  pulse on the apical side, leading to a significantly faster drop in MEQ fluorescence compared with that in the absence of  $\text{HCO}_3^-$ . Addition of 5  $\mu\text{M}$  genistein in the presence of  $\text{HCO}_3^-$  further accelerated  $\text{Cl}^-$  influx by a factor of 2 greater than the sum of the increased  $\text{Cl}^-$  flux due to genistein and  $\text{HCO}_3^-$  alone. These results, summarized in Fig. 3D, demonstrate a synergistic effect of  $\text{HCO}_3^-$  and genistein consistent with  $\text{HCO}_3^-$ -dependent increases in apical  $\text{Cl}^-$  permeability via activation of CFTR.

If  $\text{HCO}_3^-$ -activated apical  $\text{Cl}^-$  permeability is produced by stimulating sAC, then the weak agonist  $\text{HSO}_3^-$ , which reduces  $\text{HCO}_3^-$ -dependent CFTR phosphorylation (Fig. 3A), should reduce the effect. Figure 4A shows that when  $\text{Cl}^-$  was applied to the apical side in the presence of  $\text{HCO}_3^-$  and 20 mM  $\text{HSO}_3^-$ , the rate of MEQ fluorescence quenching was

reduced relative to  $HCO_3^-$  alone. Independent experiments showed that in the absence of  $HCO_3^-$ ,  $H_2SO_3$  produced a small increase (13%) in the rate of  $Cl^-$  entry (Fig. 4B, inset), consistent with a weak stimulation of sAC and the relatively small increase in CFTR phosphorylation (Fig. 3A). These results, summarized in Fig. 4B, demonstrate that  $H_2SO_3$  inhibited  $HCO_3^-$ -activated  $Cl^-$  permeability by 59%, consistent with increased apical  $Cl^-$  permeability from activation of sAC. Similarly, Fig. 4C shows that when  $Cl^-$  was applied on the apical side in the presence of  $HCO_3^-$  together with 50  $\mu$ M Rp-adenosine 3',5'-cyclic monophosphorothioate (Rp-cAMP[S]), a specific PKA inhibitor, the rate of MEQ fluorescence quenching was reduced relative to  $HCO_3^-$  alone. In separate experiments, we found that in the absence of  $HCO_3^-$ , Rp-cAMP[S] produced a small but insignificant reduction in  $Cl^-$  permeability (Fig. 4D, inset). These results, summarized in Fig. 4D, demonstrate that Rp-cAMP[S] inhibited  $HCO_3^-$ -activated  $Cl^-$  permeability by ~57%, consistent with a PKA-mediated process.

## DISCUSSION

This is the first demonstration that activation of sAC by  $HCO_3^-$  in an epithelial cell can lead to phosphorylation and activation of CFTR. The sAC- $HCO_3^-$ -induced production of cAMP represents an additional mode of signal transduction that is best described as contributing to baseline or resting conductance of CFTR, because  $HCO_3^-$  is almost always present in vivo. The increase in [cAMP] during PDE inhibition in the presence or absence of  $HCO_3^-$  (Fig. 1) indicates that sAC activity is one of possibly numerous ACs contributing to baseline cAMP production.

We show that sAC message is present in BCEC and the enzyme is distributed throughout the cytoplasm. Increased rates of cAMP formation in BCEC were [ $HCO_3^-$ ] dependent. This is consistent with previous studies demonstrating  $HCO_3^-$ -activated AC activity in particulate fractions of BCEC (28).  $HCO_3^-$  caused a 23% and 42% increase in [cAMP] in the absence and presence of PDE4 inhibition, respectively. This is modest in comparison to prototypical neural or humoral agonists (e.g., VIP; Ref. 26) or forskolin (35), which can produce a >10-fold increase in [cAMP] in the presence or absence of PDE inhibitors, respectively. However, in the absence of PDE inhibition, adenosine can stimulate cAMP-dependent fluid secretion in corneal endothelium (33) and Calu-3 airway cells (20) without significantly changing total cell [cAMP]. In the presence of PDE inhibition, adenosine significantly increased total cell [cAMP] in corneal endothelium (33), indicating that inhibition of robust PDE activity is sometimes needed to uncover increases in AC activity when total cell [cAMP] is measured. Moreover, in the absence of PDE inhibition, we show that adenosine and  $HCO_3^-$  produce significant increases in PKA-dependent phosphorylation of CFTR (Fig. 3), suggesting that each of these agonists is creating localized increases in [cAMP]. The ability of cells to sustain local [cAMP] gradients has been demonstrated (32, 48). Furthermore, recent studies showed that sAC distribution throughout the cell can be highly localized (50). Whether sAC is localized at the cell membrane in BCEC will require further study.



In the presence of  $HCO_3^-$ , sAC stimulation activates CFTR as shown by 1) a  $HCO_3^-$ -activated apical  $Cl^-$  permeability that is inhibited by NPPB, but not  $H_2DIDS$ , and is inconsistent with anion exchange or SACCs; 2) inhibition of  $HCO_3^-$ -activated apical  $Cl^-$  permeability by  $H_2SO_3^-$ , a weak agonist (and competitor with  $HCO_3^-$ ) of sAC (12), and inhibition by Rp-cAMP[S], an inhibitor of PKA; 3) increased sensitivity to 5  $\mu$ M genistein in the presence of  $HCO_3^-$ ; 4) increasing CFTR phosphorylation with increasing  $[HCO_3^-]$  that can be reduced by  $H_2SO_3^-$ ; and 5) increasing apical  $Cl^-$  permeability with increasing  $[HCO_3^-]$  that shows increasing activity in the physiological range (10–20 mM), which is consistent with an  $EC_{50}$  of ~25 mM that was determined for sAC in cell extracts (12). Other effects of  $HCO_3^-$  that may possibly influence these results include membrane potential hyperpolarization (~5 mV) from  $Na^+-2HCO_3^-$  uptake (3, 25) and a rise in  $pH_i$  by ~0.2 units (2). Hyperpolarization would reduce  $Cl^-$  entry during the apical  $Cl^-$  pulses, so our estimates of relative permeability in  $HCO_3^-$  may actually be a little low. On the other hand, increases in  $pH_i$  can increase conductance of phosphorylated CFTR in sweat glands predominantly by suppressing phosphatase activity (31). In sweat glands, a  $pH_i$  change from 7.15 to 7.35 would increase CFTR conductance by ~9% (31). However, in BCEC, a 0.2-pH unit increase from 7.12 to 7.32 did not significantly increase apical  $Cl^-$  permeability (Table 1). These results indicate that in corneal endothelium,  $HCO_3^-$  stimulates CFTR predominantly by activation of sAC. Because CFTR is also permeable to  $HCO_3^-$  in BCEC (42),  $HCO_3^-$  activation of sAC should also enhance apical  $HCO_3^-$  permeability as well as  $Cl^-$ , contributing to net transendothelial flux of both anions.

Corneal hydration changes little over the course of a day, so corneal endothelial fluid secretion *in vivo* must be continuous and relatively constant. Our results suggest that sAC- $HCO_3^-$ -dependent cAMP production provides a continuous and relatively constant source of autocrine stimulation. Another possible source of continuous autocrine stimulation is ATP release. Activated CFTR can facilitate ATP release across apical membranes (9, 11, 14). This suggests that  $HCO_3^-$ -activated sAC could contribute to constitutive ATP release. Constitutive ATP efflux occurs in unperturbed BCEC (41). ATP is converted to adenosine by ectonucleotidases on the apical surface of BCEC (37), and adenosine binds to  $A_{2B}$  receptors stimulating cAMP production (33), which in turn activates PKA and CFTR (3, 49). The resultant membrane voltage depolarization (3) maintains basolateral  $Na^+-2HCO_3^-$  cotransporter uptake, thereby reinforcing  $HCO_3^-$  uptake and sAC activity. Thus the sAC and adenosine signaling pathways may be functionally linked. This is illustrated in Fig. 5, in which we suggest a signaling model that coordinates the actions of the sAC and adenosine autocrine signaling pathways for maintenance of baseline CFTR conductance in the corneal endothelium.

In conclusion, we have demonstrated in corneal endothelial cells that sAC expression and activation by  $HCO_3^-$  can increase [cAMP], leading to phosphorylation of apical CFTR with a concomitant increase in apical  $Cl^-$  permeability. Because the corneal endothelium is not innervated and is shielded from humoral agonists, this form of sustained autocrine stimulation may be important for the small ( $4 \mu\text{l}\cdot\text{cm}^{-2}\cdot\text{h}^{-1}$ ) but constant fluid secretion of this epithelium. In addition to  $HCO_3^-$  flux contributing to net anion flux in corneal

endothelium, we must add that  $\text{HCO}_3^-$  is a sAC agonist, contributing indirectly to baseline cAMP-dependent ion transport.

## Acknowledgments

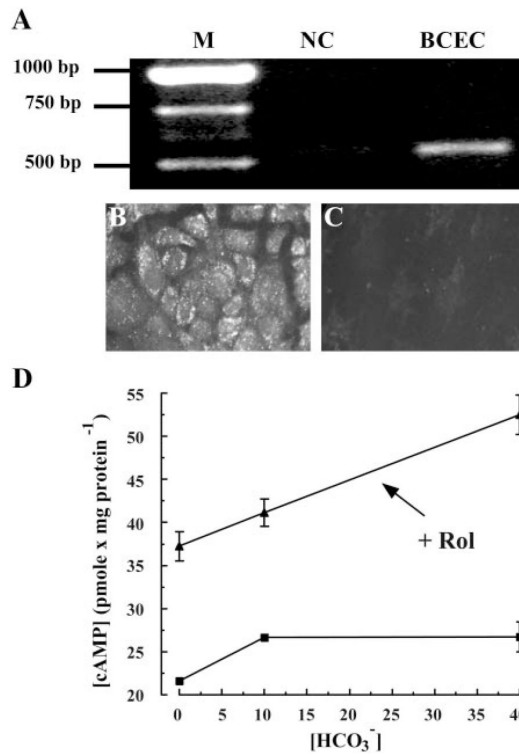
This study was supported by National Institutes of Health Grants EY-08834 (J. A. Bonanno), HD-38722 (L. R. Levin), GM-62328 (J. Buck), and HD-42060 (J. Buck).

## REFERENCES

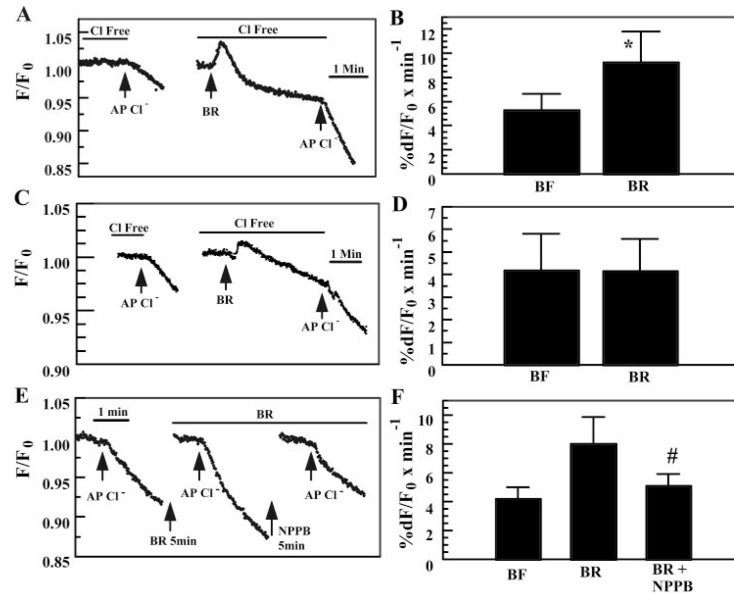
1. Al-Nakkash L, Hu S, Li M, Hwang TC. A common mechanism for cystic fibrosis transmembrane conductance regulator protein activation by genistein and benzimidazolone analogs. *J Pharmacol Exp Ther.* 2001; 296:464–472. [PubMed: 11160632]
2. Bonanno J, Guan Y, Jelamskii S, Kang X. Apical and basolateral  $\text{CO}_2\text{-HCO}_3^-$  permeability in cultured bovine corneal endothelial cells. *Am J Physiol Cell Physiol.* 1999; 277:C545–C553.
3. Bonanno J, Srinivas S. Cyclic AMP activates anion channels in cultured bovine corneal endothelial cells. *Exp Eye Res.* 1997; 64:953–962. [PubMed: 9301476]
4. Bonanno JA, Giasson C. Intracellular pH regulation in fresh and cultured bovine corneal endothelium. I. Na/H exchange in the absence and presence of  $\text{HCO}_3^-$ . *Invest Ophthalmol Vis Sci.* 1992; 33:3058–3067. [PubMed: 1328110]
5. Bonanno JA, Giasson C. Intracellular pH regulation in fresh and cultured bovine corneal endothelium. II. Na: $\text{HCO}_3^-$  cotransport and  $\text{Cl}^-/\text{HCO}_3^-$  exchange. *Invest Ophthalmol Vis Sci.* 1992; 33:3068–3079. [PubMed: 1399410]
6. Bonanno JA, Srinivas SP, Brown M. Effect of acetazolamide on intracellular pH and bicarbonate transport on bovine corneal endothelium. *Exp Eye Res.* 1995; 60:425–434. [PubMed: 7789422]
7. Bonanno JA, Yi G, Kang XJ, Srinivas SP. Reevaluation of  $\text{Cl}^-/\text{HCO}_3^-$  exchange in cultured bovine corneal endothelial cells. *Invest Ophthalmol Vis Sci.* 1998; 39:2713–2722. [PubMed: 9856782]
8. Braun T. Purification of soluble form of adenylyl cyclase from testes. *Methods Enzymol.* 1991; 195:130–136. [PubMed: 1851925]
9. Braunstein GM, Roman RM, Clancy JP, Kudlow BA, Taylor AL, Shylonsky VG, Jovov B, Peter K, Jilling T, Ismailov II, Benos DJ, Schwiebert LM, Fitz JG, Schwiebert EM. Cystic fibrosis transmembrane conductance regulator facilitates ATP release by stimulating a separate ATP release channel for autocrine control of cell volume regulation. *J Biol Chem.* 2001; 276:6621–6630. [PubMed: 11110786]
10. Buck J, Sinclair ML, Schapal L, Cann MJ, Levin LR. Cytosolic adenylyl cyclase defines a unique signaling molecule in mammals. *Proc Natl Acad Sci USA.* 1999; 96:79–84. [PubMed: 9874775]
11. Cantiello F. Electrodifusional ATP movement through CFTR and other ABC transporters. *Pflügers Arch.* 2001; 443:S22–S27. [PubMed: 11845298]
12. Chen Y, Cann MJ, Litvin TN, Iourgenko V, Sinclair ML, Levin LR, Buck J. Soluble adenylyl cyclase as an evolutionarily conserved bicarbonate sensor. *Science.* 2000; 289:625–628. [PubMed: 10915626]
13. Diecke F, Zhu Z, Kang F, Kuang K, Fischbarg J. Sodium, potassium, two chloride cotransport in corneal endothelium: characterization and possible role in volume regulation and fluid transport. *Invest Ophthalmol Vis Sci.* 1998; 39:104–110. [PubMed: 9430551]
14. Egan M. CFTR-associated ATP transport and release. *Methods Mol Med.* 2002; 70:395–406. [PubMed: 11917539]
15. Fischbarg J, Lim J. Role of cations, anions, and carbonic anhydrase in fluid transport across rabbit corneal endothelium. *J Physiol.* 1974; 241:647–675. [PubMed: 4215880]
16. Fischbarg J, Lim J, Bourguet J. Adenosine stimulation of fluid transport across rabbit corneal endothelium. *J Membr Biol.* 1977; 35:95–112. [PubMed: 886607]
17. Goddard CA, Evans MJ, Colledge WH. Genistein activates CFTR-mediated  $\text{Cl}^-$  secretion in the murine trachea and colon. *Am J Physiol Cell Physiol.* 2000; 279:C383–C392. [PubMed: 10913005]

18. Hodson S. The regulation of corneal hydration by a salt pump requiring the presence of sodium and bicarbonate ions. *J Physiol.* 1974; 236:271–302. [PubMed: 16992435]
19. Hodson S, Miller F. The bicarbonate ion pump in the endothelium which regulates the hydration of rabbit cornea. *J Physiol.* 1976; 263:563–577. [PubMed: 828203]
20. Huang P, Lazarowski ER, Tarran R, Milgram SL, Boucher RC, Stutts MJ. Compartmentalized autocrine signaling to cystic fibrosis transmembrane conductance regulator at the apical membrane of airway epithelial cells. *Proc Natl Acad Sci USA.* 2001; 98:14120–14125. [PubMed: 11707576]
21. Huff J, Green K. Characteristics of bicarbonate, sodium, and chloride fluxes in the rabbit corneal endothelium. *Exp Eye Res.* 1983; 36:607–615. [PubMed: 6852135]
22. Illek B, Fischer H. Flavonoids stimulate Cl conductance of human airway epithelium in vitro and in vivo. *Am J Physiol Lung Cell Mol Physiol.* 1998; 275:L902–L910.
23. Jelamskii S, Sun XC, Herse P, Bonanno JA. Basolateral Na<sup>+</sup>-K<sup>+</sup>-2Cl<sup>-</sup> cotransport in cultured and fresh bovine corneal endothelium. *Invest Ophthalmol Vis Sci.* 2000; 41:488–495. [PubMed: 10670480]
24. Jentsch T, Keller S, Koch M, Wiederholt M. Evidence for coupled transport of bicarbonate and sodium in cultured bovine corneal endothelial cells. *J Membr Biol.* 1984; 81:189–204. [PubMed: 6502693]
25. Jentsch TJ, Koch M, Bleckmann H, Weiderholt M. Effect of bicarbonate, pH, Methazolamide and stilbenes on the intracellular potentials of cultured bovine corneal endothelial cells. *J Membr Biol.* 1984; 78:103–117. [PubMed: 6325699]
26. Koh SW, Yue BY. VIP stimulation of cAMP production in corneal endothelial cells in tissue and organ cultures. *Cornea.* 2002; 21:270–274. [PubMed: 11917175]
27. Kuang K, Xu M, Koniarek J, Fischbarg J. Effects of ambient bicarbonate, phosphate and carbonic anhydrase inhibitors on fluid transport across rabbit endothelium. *Exp Eye Res.* 1990; 50:487–493. [PubMed: 2373152]
28. Mittag TW, Guo WB, Kobayashi K. Bicarbonate-activated adenylyl cyclase in fluid-transporting tissues. *Am J Physiol Renal Fluid Electrolyte Physiol.* 1993; 264:F1060–F1064.
29. Nilius B, Droogmans G. Ion channels and their functional role in vascular endothelium. *Physiol Rev.* 2001; 81:1415–1459. [PubMed: 11581493]
30. Ransom CB, O’Neal JT, Sontheimer H. Volume-activated chloride currents contribute to the resting conductance and invasive migration of human glioma cells. *J Neurosci.* 2001; 21:7674–7683. [PubMed: 11567057]
31. Reddy MM, Kopito RR, Quinton PM. Cytosolic pH regulates G<sub>Cl</sub> through control of phosphorylation states of CFTR. *Am J Physiol Cell Physiol.* 1998; 275:C1040–C1047.
32. Rich TC, Fagan KA, Tse TE, Schaack J, Cooper DM, Karpen JW. A uniform extracellular stimulus triggers distinct cAMP signals in different compartments of a simple cell. *Proc Natl Acad Sci USA.* 2001; 98:13049–13054. [PubMed: 11606735]
33. Riley M, Winkler B, Starnes C, Peters M. Adenosine promotes regulation of corneal hydration through cyclic adeno-sine monophosphate. *Invest Ophthalmol Vis Sci.* 1996; 37:1–10. [PubMed: 8550312]
34. Riley M, Winkler B, Starnes C, Peters M. Fluid and ion transport in corneal endothelium: insensitivity to modulators of Na-K-2Cl cotransport. *Am J Physiol Cell Physiol.* 1997; 273:C1480–C1486.
35. Riley MV, Winkler BS, Starnes CA, Peters MI, Dang L. Regulation of corneal endothelial barrier function by adenosine, cyclic AMP, and protein kinases. *Invest Ophthalmol Vis Sci.* 1998; 39:2076–2084. [PubMed: 9761286]
36. Sinclair ML, Wang X, Melissa M, Conti M, Buck J, Wolgemuth DJ, Levin LR. Specific expression of soluble adenylyl cyclase in male germ cells. *Mol Reprod Dev.* 2000; 56:6–11. [PubMed: 10737962]
37. Soltau J, Zhou L, McLaughlin B. Isolation of plasma membrane domains from bovine corneal endothelial cells. *Exp Eye Res.* 1993; 115–120. [PubMed: 8381748]
38. Srinivas SP, Bonanno JA. Measurement of changes in cell volume based on fluorescence quenching. *Am J Physiol Cell Physiol.* 1997; 272:C1405–C1414.

39. Srinivas SP, Bonanno JA, Hughes BA. Assessment of swelling-activated  $\text{Cl}^-$  channels using the halide-sensitive fluorescent indicator 6-methoxy-*n*-(3-sulfopropyl)quinolinium. *Biophys J*. 1998; 75:115–123. [PubMed: 9649372]
40. Srinivas SP, Guan Y, Bonanno JA. Swelling activated chloride channels in cultured bovine corneal endothelial cells. *Exp Eye Res*. 1999; 68:165–177. [PubMed: 10068482]
41. Srinivas SP, Mutharasan R, Sun XC, Bonanno JA. Stretch-activated ATP release by corneal endothelium. *Invest Ophthalmol Vis Sci*. 2001; 42:S665.
42. Sun XC, Bonanno JA. Expression, localization, and functional evaluation of CFTR in bovine corneal endothelial cells. *Am J Physiol Cell Physiol*. 2002; 282:C673–C683. [PubMed: 11880256]
43. Sun XC, Bonanno JA, Jelamskii S, Xie Q. Expression and localization of  $\text{NaHCO}_3$  cotransporter in bovine corneal endothelium. *Am J Physiol Cell Physiol*. 2000; 279:C1648–C1655. [PubMed: 11029313]
44. Sun XC, McCutcheon C, Bertram P, Xie Q, Bonanno JA. Studies on the expression of mRNA for anion transport related proteins in corneal endothelial cells. *Curr Eye Res*. 2001; 22:1–7. [PubMed: 11402373]
45. Wigham C, Hodson S. The movement of sodium across short-circuited rabbit corneal endothelium. *Curr Eye Res*. 1985; 4:1241–1245. [PubMed: 4085251]
46. Wigham CG, Turner HC, Swan J, Hodson SA. Modulation of corneal endothelial hydration control mechanisms by Rolipram. *Pflügers Arch*. 2000; 440:866–870. [PubMed: 11041552]
47. Winkler B, Riley M, Peters M, Williams F. Chloride is required for fluid transport by the rabbit corneal endothelium. *Am J Physiol Cell Physiol*. 1992; 262:C1167–C1174.
48. Zaccolo M, Pozzan T. Discrete microdomains with high concentration of cAMP in stimulated rat neonatal cardiac myocytes. *Science*. 2002; 295:1711–1715. [PubMed: 11872839]
49. Zhang Y, Xie Q, Sun XC, Bonanno JA. Enhancement of  $\text{HCO}_3^-$  permeability across the apical membrane of bovine corneal endothelium by multiple signaling pathways. *Invest Ophthalmol Vis Sci*. 2002; 43:1146–1153. [PubMed: 11923259]
50. Zippin JH, Chen Y, Nahirney P, Kamenetsky M, Wuttke MS, Fischman DA, Levin LR, Buck J. Compartmentalization of bicarbonate-sensitive adenylyl cyclase in distinct signaling microdomains. *FASEB J*. 2003; 17:82–84. [PubMed: 12475901]

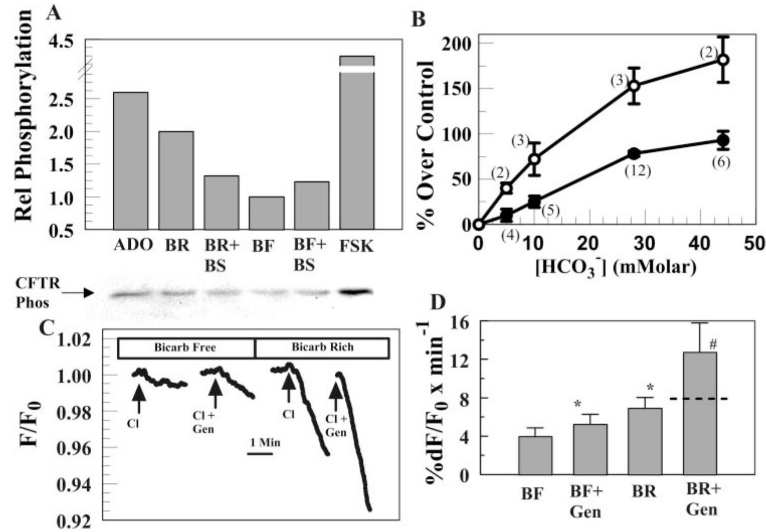


**Fig. 1.** Expression of  $HCO_3^-$ -activated soluble adenylyl cyclase (sAC) in corneal endothelium. **A**: RT-PCR for sAC. M, markers; BCEC, cultured bovine corneal endothelial cells; NC, negative control (no RT). **B** and **C**: indirect immunofluorescence for sAC in cultured BCEC. **B**: primary sAC antibody. **C**: no sAC antibody. **D**:  $HCO_3^-$ -activated intracellular cAMP concentration ([cAMP]) in BCEC. Cells were incubated in  $HCO_3^-$ -free DMEM at 37°C for 3 h and then for 30 min in 0.3 mM  $\alpha,\beta$ -methyleneadenosine 5'-diphosphate (AMP-CP) at different  $[HCO_3^-]$ , with ( $\blacktriangle$ ) or without ( $\blacksquare$ ) 50  $\mu$ M rolipram (Rol). Error bars indicate  $\pm$ SE ( $n = 6$ ).



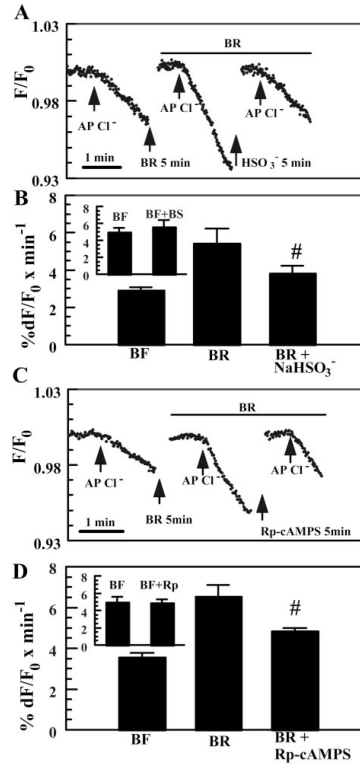
**Fig. 2.**

Effect of  $HCO_3^-$  on apical  $Cl^-$  permeability in BCEC and CHO cells. **A:** BCEC. Both apical and basolateral compartments were initially perfused with  $Cl^-$ - and  $HCO_3^-$ -free Ringer solution. After the 1st apical (AP)  $Cl^-$  pulse,  $HCO_3^-$ -rich Ringer solution (BR) was introduced on both sides for at least 5 min before the 2nd  $Cl^-$  pulse. Break in trace indicates period of wash in  $Cl^-$ -free solution until trace stabilized (at least 5 min). **B:** summary data for A; all fluorescence values were normalized to the fluorescence value in the absence of  $Cl^-$  ( $F_0$ ) obtained just before addition of  $Cl^-$ . Calculated slopes were adjusted by any background drift in the fluorescence trace that was apparent just before addition of  $Cl^-$ . \*Significantly different from  $HCO_3^-$  free solution (BF) ( $n = 11$ ;  $P < 0.05$ ). **C:** CHO cells, same experiment as in A. **D:** summary data for C ( $n = 7$ ). **E:** effect of 5-nitro-2-(3-phenylpropyl-amino)benzoic acid (NPPB) on  $HCO_3^-$ -activated apical  $Cl^-$  permeability in BCEC. **F:** summary data for E. #Significantly different from BR ( $n = 8$ ,  $P < 0.05$ ).



**Fig. 3.**

The presence of  $HCO_3^-$  increases phosphorylation and sensitizes cystic fibrosis transmembrane conductance regulator (CFTR) to genistein. *A*, bottom: blot of phosphorylated CFTR from cells incubated in 10  $\mu$ M adenosine (Ado), 28.5 mM  $HCO_3^-$  (BR), 28.5 mM  $HCO_3^-$  + 20 mM  $H_2SO_3^-$  (BR + BS), 0  $HCO_3^-$  (BF), 0  $HCO_3^-$  + 20 mM  $H_2SO_3^-$  (BF + BS), or 10  $\mu$ M forskolin (FSK). *A*, top: relative CFTR phosphorylation from blot. *B*: ○, %increase in CFTR phosphorylation after incubation in varying  $[HCO_3^-]$  relative to 0  $HCO_3^-$ ; ●, increase in apical  $Cl^-$  permeability relative to 0  $HCO_3^-$ . Data points are means  $\pm$  SE; nos. in parentheses indicate the no. of trials. *C*: effect of 5  $\mu$ M genistein (Gen) on  $HCO_3^-$ -activated  $Cl^-$  permeability in 0.3 mM AMP-CP-treated cells. Breaks in trace indicate periods of wash in  $Cl^-$ -free solution. *D*: summary data for *C*. \*Significantly different from BF ( $n = 10$ ,  $P < 0.05$ ). #Increment over BF is significantly greater than the sum of the increased rates over BF due to BF + Gen plus BR (indicated by dashed line in BR + Gen bar) ( $n = 10$ ,  $P < 0.05$ ).

**Fig. 4.**

Inhibition of sAC and PKA reduces  $HCO_3^-$ -activated apical  $Cl^-$  permeability. *A*: effect of the weak sAC agonist  $HSO_3^-$  (20 mM) on apical  $Cl^-$  permeability. Bisulfite solutions were prepared by adding 20 mM  $NaHSO_3$  directly to  $Cl^-$ -free and  $HCO_3^-$ -rich solutions. Equimolar Na-gluconate was added to all other solutions. Osmolality was within  $\pm 5$  mosmol/kgH<sub>2</sub>O for all solutions. Breaks in the trace indicate periods of  $Cl^-$ -free wash (at least 5 min). *B*: summary data for *A*. <sup>#</sup>Significantly different from BR ( $n = 5$ ,  $P < 0.05$ ). *Inset*: independent experiments comparing apical  $Cl^-$  permeability in  $HCO_3^-$ -free Ringer solution (BF) with or without  $HSO_3^-$  (BS). *C*: inhibition of  $HCO_3^-$ -activated apical  $Cl^-$  permeability by the PKA inhibitor Rp-adenosine 3',5'-cyclic monophosphorothioate (Rp-cAMP[S]; 50  $\mu$ M). *D*: summary data for *C*. <sup>#</sup>Different from BR ( $n = 5$ ,  $P < 0.05$ ). *Inset*: independent experiments comparing apical  $Cl^-$  permeability in  $HCO_3^-$ -free Ringer solution with or without Rp-cAMP[S].



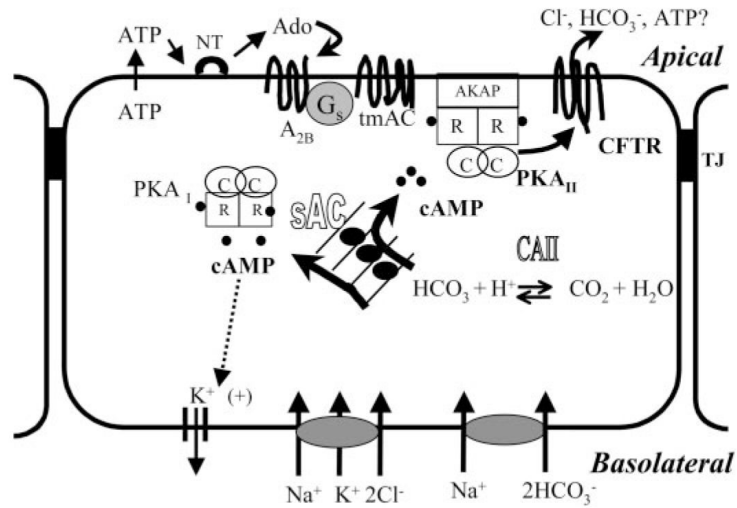


**Fig. 5.** Model for the role of sAC in anion transport signaling in corneal endothelium. Basolateral  $\text{Na}^+\text{-K}^+\text{-2Cl}^-$  and  $\text{Na}^+\text{-2HCO}_3^-$  cotransporters load  $\text{Cl}^-$  and  $\text{HCO}_3^-$ , respectively, into corneal endothelial cells.  $\text{HCO}_3^-$  stimulates sAC, producing cAMP throughout the cell, activating PKA I, PKA II, and possibly cAMP-dependent  $\text{K}^+$  channels. The activation of apical CFTR enhances anion efflux. Activated CFTR facilitates ATP release across the apical membrane. ATP is converted to adenosine (Ado) by ectonucleotidases (NT). Adenosine binds to A2B receptors, stimulating local cAMP production and phosphorylation of CFTR via PKA II. Any form of stimulated apical anion efflux depolarizes the membrane voltage, thereby increasing the driving force for basolateral  $\text{Na}^+\text{-2HCO}_3^-$  cotransport and maintenance of sAC stimulation. TJ, tight junction; CAII, carbonic anhydrase II; tmAC, transmembrane AC; AKAP, A-kinase-anchoring protein; R and C, regulatory and catalytic subunits, respectively.

**Table 1**Effect of  $\text{pH}_i$  on relative apical  $\text{Cl}^-$  permeability

Bath pH ( $\text{HCO}_3^-$ free)	Measured $\text{pH}_i$ (n = 3)	Relative Apical $\text{Cl}^-$ Permeability (n = 6)
7.00	6.88±0.07	0.89±0.03
7.50	7.12±0.05	1.0±0.08
8.00	7.32±0.08	1.02±0.03

Intracellular pH ( $\text{pH}_i$ ) and  $\text{Cl}^-$  permeability values are means  $\pm$  SE. Bovine corneal endothelial cells (BCEC) were loaded with the pH-sensitive fluorescent dye BCECF, and  $\text{pH}_i$  was measured while perfused at pH 7.0, 7.5, and 8.0 in the absence of  $\text{HCO}_3^-$ . In separate experiments, cells were loaded with 6-methoxy-*N*-ethylquinolinium iodide (MEQ), and apical  $\text{Cl}^-$  permeability was measured (see MATERIALS AND METHODS) at the 3 bath pH levels in the absence of  $\text{HCO}_3^-$ .  $\text{Cl}^-$  permeability values are relative to control (bath pH 7.50).